



DEVELOPMENT OF METHOD FOR EVALUATION OF BONE STABILITY BY X-RAY PHOTOGRAPHS

Kenji Gomi¹, Akihumi Ogawara², Shota Mori¹, Saiko Yamaki¹, Ryuji Mori³, Takahumi Kajitani³,
Yasushi Niitsu⁴ and Kensuke Ichinose¹

¹ Department of Mechanical Engineering, Tokyo Denki University, Tokyo, JAPAN, kenji@cck.dendai.ac.jp

² Graduate School of Tokyo Denki University, Tokyo, JAPAN

³ School of Medicine, Shimane University, Shimane, JAPAN

⁴ School of Information Environment, Tokyo Denki University, Chiba, JAPAN

Abstract: Determination of the human bone stability is very important when arranging for rehabilitation or removal of internal fixators for broken bones. Usually, to determine the bone stability, doctors inspect X-ray photographs by subjectively with their experiences. As a result, it is difficult to explain quantitatively the condition to patients. Thus, a clinically feasible method to determine the bone stability is awaited. We have attempted to develop such a method for quantitative evaluation of the stability by image processing X-ray photographs. As a result, we successfully established the necessary conditions for quantitative evaluation of the bone stability.

Keywords: human bone stability, similarity method, edge detection, computer radiography system

1. INTRODUCTION

One of the operative treatments for broken bones is splinting using internal fixators. The stability of the bones is essential in arranging the rehabilitation or removal of internal fixators for the broken bones. However, the stability is generally determined by surgeons subjectively with their experiences by inspecting X-ray photographs [1]. Therefore, a quantitative evaluation method has been required to determine the stability [2]. Maffulli et al. found a relationship between the intensity changes of ultrasonographic images and the forms of bony calluses [3]. Nakatsuchi et al. developed diagnostic equipment for bony calluses by using characteristic frequency [4] [5]. However, these methods do not make it clear whether the bony calluses regain their normal strength or not [6]. Thus, we have tried to develop quantitative evaluation methods for the strength, or the stability, by image processing of X-ray photographs [7].

In this paper, the bone stability of a porcine tibia was measured using our equipment, and the necessary conditions were obtained for quantitative evaluation of the bone stability.

2. BONE STABILITY EVALUATION PRINCIPLE

2.1. Definition of stability

Figure 1 shows a schematic diagram of a fixated fracture using an internal fixator. As shown in Equation (1), the definition of the bone stability here is the strain in "B" region divided by the strain in "A" region in Figure 1: region "A" contains healthy bone and bony callus or bone union region, whereas region "B" contains healthy bone only. Note that the bony callus means the fracture cure-in-process.

$$\text{Bone stability} = \frac{\text{Strain in "B"}}{\text{Strain in "A"}} \quad (1)$$

For example, if the strain in "A" and "B" are equal, the bony callus should regain its mechanical strength completely. Generally, internal fixators are used for keeping broken bones in position while it mends by screw clamping as shown in Figure 1. Therefore, the strain in bone is obtained using screw displacements that are detected by image processing. In this paper, the following two types of image processing are tried and compared.

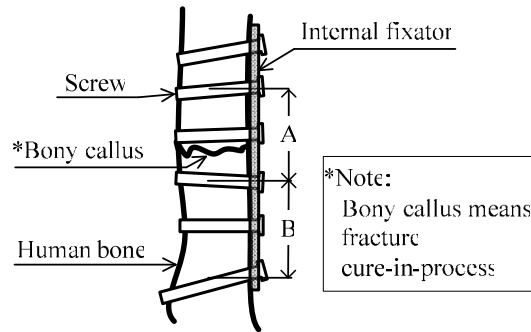


Figure 1: Schematic diagram of a fixed fracture by using an internal fixator

2.2. Displacement measurement by similarity method

The similarity method is a pattern matching method with the following procedure. (a) Define some pixels, $m \times n$, as a ROI (region of interest) in an X-ray photograph taken while unloading onto an object. (b) Define the luminance distribution of the ROI as the “ $m \times n$ ”-dimensional vector \vec{r}_1 . (c) Find the “ $m \times n$ ”-area in the X-ray photograph taken while loading on the object so that κ is proximate to 1 ($\kappa \approx 1$) in the following Equation (2):

$$\kappa = \frac{\vec{r}_1 \cdot \vec{r}_2}{|\vec{r}_1| |\vec{r}_2|} \quad (2)$$

where \vec{r}_2 is the “ $m \times n$ ”-dimensional vector corresponding to the “ $m \times n$ ”-area that is found in the procedure (c).

2.3. Displacement measurement by edge detection

Edge detection is a filtering method. The finite difference of second order is used here for detecting the boundary between the screws and bone. Equation (3) shows a finite difference of the first order:

$$f'(a) \approx \frac{f(a+h) - f(a)}{h} \quad (3)$$

3. COMPUTED RADIOGRAPHY SYSTEM

Figure 2 shows an object and general X-ray equipment called a CR (computed radiography system). An X-ray generated by an X-ray generator at the left in Figure 2 passes through an object and projects the image on an IP (imaging plate) to the right of the object. The luminance distribution is digitized by an image reading system, and then the digital image data are stored in a PC.

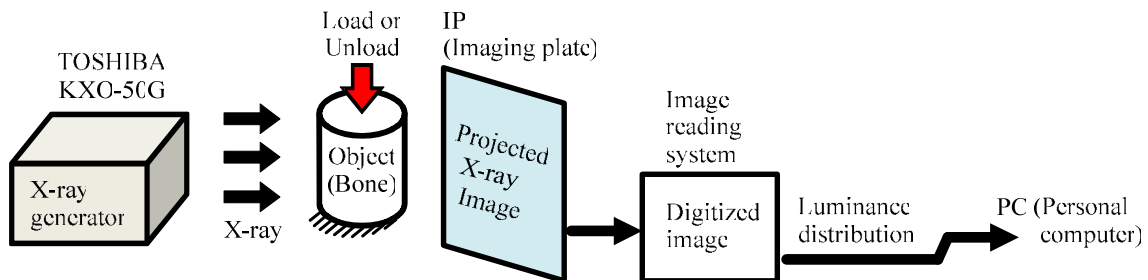


Figure 2: Schematic figure of CR (Computed radiography system)
FUJI FCR VELOCITY U

4. SPECIMEN AND EXPERIMENTAL PROCEDURES

4.1. Specimen overview

Figure 3 shows the specimen during operation for fixation with an internal fixator. The specimen whose end is held by the vice is the porcine metaphysis of a tibia (a six-month-old male Cambrough at puberty, that Young's modulus corresponds to a human adult; body weight: 110-120 kg). The specimen is amputated at the proximal part of the tibia, or at the subgenual joint, horizontally. A weight of 17.5 kg is put on the amputated plane to apply axial force to the specimen to measure the strain in the bone. The weight, 17.5 kg, was determined as the clinically maximum load by a surgeon who is the one of the authors of this paper.

4.2. Specimen “a”, complete cure model

Figure 4(a) at left shows a model of a complete cure. This is made by fixating the unbroken tibia specimen with an internal fixator. Clinically, this is six months after operation; surgeons must keep in mind that the patient must be able to return to sports activities with the internal fixator on her/his bone.

4.3. Specimen “b”, partial cure model

Figure 4(b) shows a model of a partial cure made by sawing the complete cure model until the bone is cut through to about two-thirds of the thickness from the other side of the fixator. Clinically, this is two months after operation; the fracture bone unites only in the vicinity of the fixator.

4.4. Experimental procedure

The following is the experimental procedure. (A) As shown in Figure 5(i), an X-ray photograph is taken of the unloaded complete cure model as shown in Figure 4(a). (B) As shown in Figure 5(ii), another X-ray photograph is taken of the complete cure model during loading along the bone lengthwise direction. (C) The distances between the screws in the two X-ray photographs of abovementioned step (A) and (B) are given by image processing already given. Then, the strains are calculated between the screws. (D) The bone stability of the model is calculated using Equation (1). (E) The procedure (A)-(D) is then conducted with the partial cure model. (F) Next, the bone stability of complete and partial

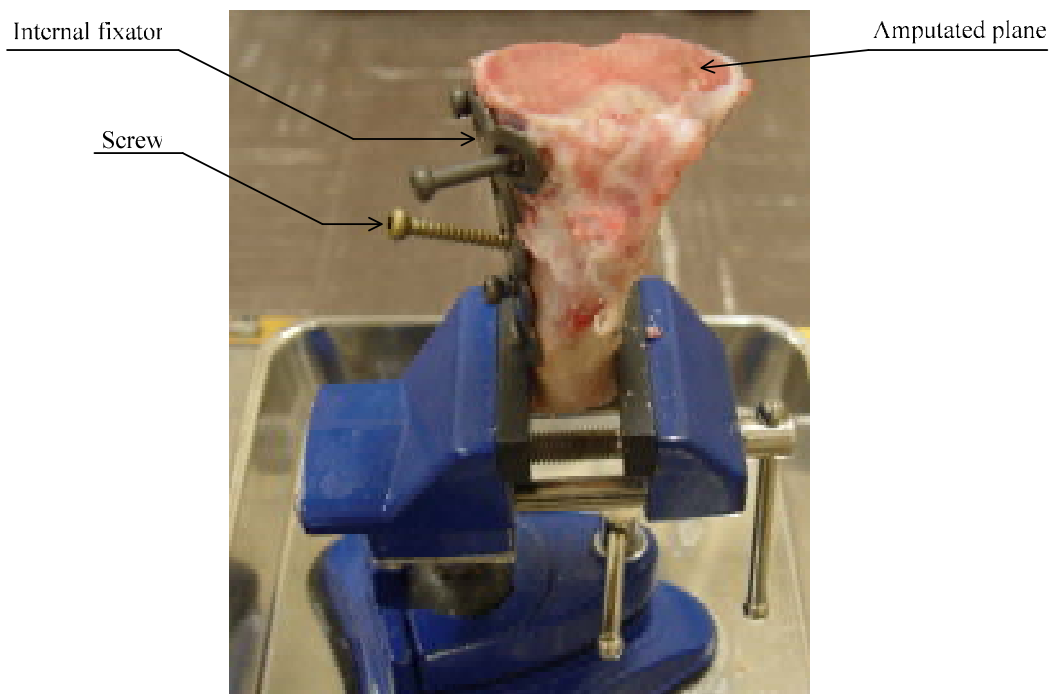


Figure 3: Specimen during operation for fixing with an internal fixator

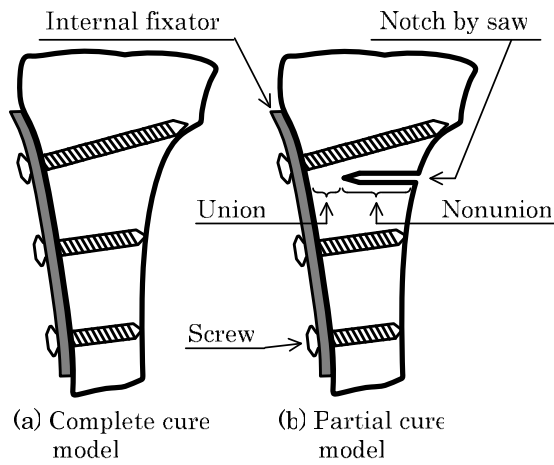
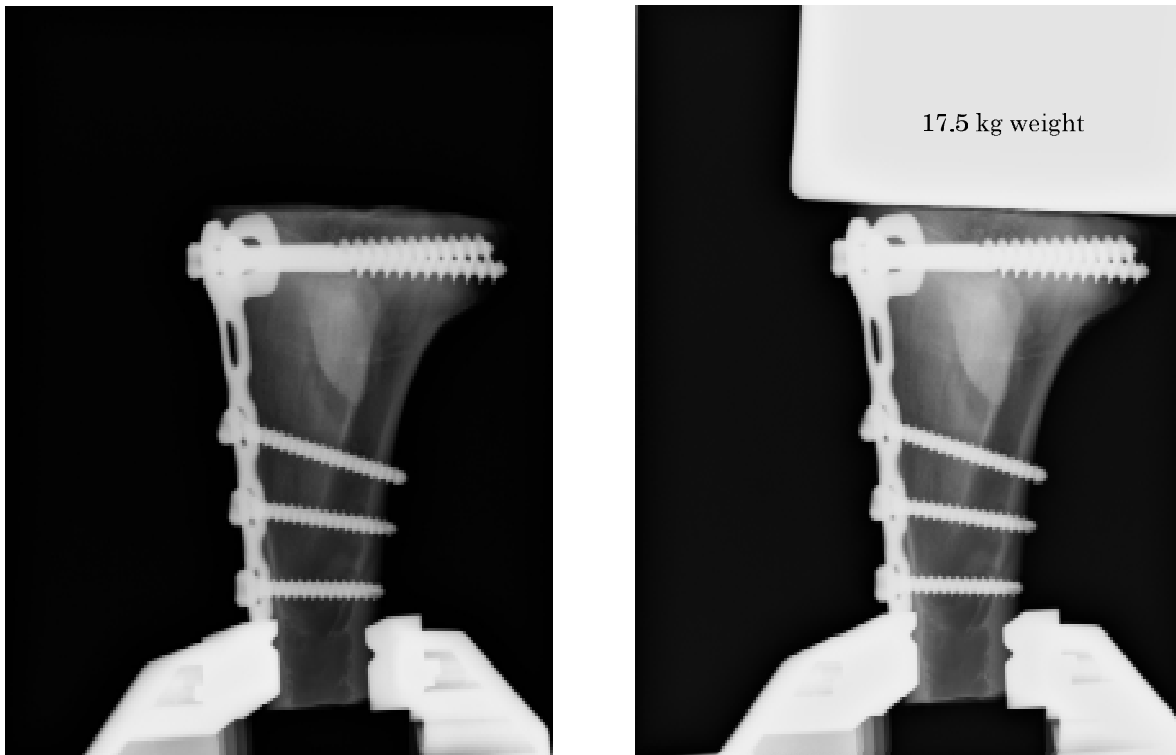


Figure 4: Schematic diagram of specimens:
 (a) complete cure model
 (b) partial cure model



(i) Specimen under no load

(ii) Specimen under load

Figure 5: X-ray photographs of specimen:
 (i) under no load
 (ii) load weight of 17.5 kg

Table 1: Results of bone stability by similarity method

	Type of models	
	Complete cure	Partial cure
Stability	1.00	1.00

Table 2: Results of bone stability by edge detection

	Type of models	
	Complete cure	Partial cure
Stability	0.984	0.997

cure models are compared and discussed. Note that the bone stability is not always 1 even with the complete cure model because of the mechanical and geometrical anisotropy of bones. Therefore, the time variation of the stability has a meaning; in other words, clinically, the progress of the cure is estimated by the increase rate of the stability.

5. RESULTS AND DISCUSSION

Table 1 shows the bone stability of the complete and partial cure models by the similarity method, while Table 2 shows the stability by edge detection. Generally, the stability of the complete cure model will be greater than that of the partial cure model. However, as shown in Table 1, the stabilities were the same by either model with the similarity method. As shown in Table 2, the stability of the complete cure model was less than that of the partial cure model with edge detection.

Since the applied load with 17.5 kgf as the clinically maximum load, is not enough to detect the displacement of the screws, it is considered as one of the factors causing problems. Generally, the detectable minimum displacement for image processing is said to be one-tenth of a pixel. Accordingly, the minimum load, P , to obtain the stability is derived by Equation (4):

$$\begin{aligned}
 P &= AE\varepsilon \\
 &= \left(\frac{5}{10^4} [m^2]\right) \times \left(\frac{20 \times 10^9}{9.81} [kgf / m^2]\right) \times \left(\frac{1/10}{1000}\right) \\
 &= 100 [kgf]
 \end{aligned} \tag{4}$$

where A is the cross-sectional area of the tibia, E is Young's modulus of the tibia, and ε is the detectable minimum strain, respectively. From the solution to Equation (4), it was found that the applied load, 17.5 kgf, was not enough to determine the stability. This problem is solved by improving the resolving power of sub-pixel of the image processing methods or focusing on softer bones of infants. Generally, Young's modulus of the bones of infants is about one-tenth of that of adults. In that case, the required minimum load will be about one-tenth of P in Equation (4).

6. CONCLUSION

The bone stability of a porcine tibia was measured using image processing with digital X-ray photographs. By meeting the following conditions, the stability of human bone may be determined:

- (I) improving the resolving power of sub-pixel of image processing methods

(II) focusing on infant bones, which have generally one-tenth Young's modulus compared with that of adult bones

ACKNOWLEDGMENTS

A part of this research was supported by Research for Promoting Technological Seeds, No. 04-135, from the Japan Science and Technology Agency, Tokyo Denki University Science Promotion Fund and Funai Foundation for Information Technology.

REFERENCES

- [1] Sakai, R., et al.: Development of a new ultrasound method for quantitative assessment of mechanical properties of bone healing, *Jpn. J. Med. Ultrasonics*, 34 Supplement, 2007, p.S562 (in Japanese).
 - [2] Kawasaki, Y., et al.: Influence of solid phase distribution in articular cartilage on ultrasonic echo, *Proceedings of the 2004 Annual Meeting of the Japan Society of Mechanical Engineers*, 2004, pp.107-108 (in Japanese).
 - [3] Maffulli, N., et al.: Ultrasonographic monitoring of limb lengthening, *J Bone Joint Surg (Br.)*, 1992, pp.130-132.
 - [4] Nakatsuchi, Y.: Measurement method and equipment of bone strength, Japanese Patent Disclosure H11-169352, 1999 (in Japanese).
 - [5] Japan Science and Technology Agency: Success in development of diagnostic equipment for callus by using characteristic frequency, Reports of Japan Science and Technology Corporation Press Release No. 115. (online), available from <<http://www.jst.go.jp/pr/report/report115/>>, (accessed 2009-3-31) (in Japanese).
 - [6] Takanaga, Y.: Equipment for measurement of bone strength, Japanese Patent Disclosure H8-182681, 1996 (in Japanese).
 - [7] Endo, H., et al.: Development of evaluation method of strain in bones applying digital correlation method, *Proceedings of the 48th Kanto Branch Annual Student Meeting of the Japan Society of Mechanical Engineers*, 2009, pp.51-52 (in Japanese).
-